Available online at www.sciencedirect.com
SCIENCE DIRECT®
Colloids and Surfaces B: Biointerfaces 40 (2005) 159–163
COLLOIDS AND SURFACES B
www.elsevier.com/locate/colsurfb

Neutron and X-ray scattering studies of cholera toxin interactions with lipid monolayers at the air–liquid interface

C.E. Miller[a], J. Majewski[b,*], K. Kjær[c], M. Weygand[c], R. Faller[e], S. Satija[d], T.L. Kuhl[e]

[a] *Biophysics Graduate Group, University of California, Davis, CA 95616, USA*
[b] *Manuel Lujan Neutron Scattering Center, Los Alamos National Laboratory, Los Alamos, NM 87545, USA*
[c] *Physics Department, Risø National Laboratory, DK-4000 Roskilde, Denmark*
[d] *Center for Neutron Research, National Institute of Standards and Technology, Gaithersburg, MD 20899, USA*
[e] *Department of Chemical Engineering and Materials Science, University of California, Davis, California, CA 95616, USA*

Available online 8 December 2004

Abstract

Using neutron/X-ray reflectivity and X-ray grazing incidence diffraction (GID), we have characterized the structure of mixed DPPE:GM_1 lipid monolayers before and during the binding of cholera toxin ($CTAB_5$) or its B subunit (CTB_5). Structural parameters such as the density and thickness of the lipid layer, extension of the GM_1 oligosaccharide headgroup, and orientation and position of the protein upon binding are reported. Both $CTAB_5$ and CTB_5 were measured to have ∼50% coverage when bound to the lipid monolayer. X-ray GID experiments show that both the lipid monolayer and the cholera toxin layer are crystalline. The effects of X-ray beam damage have been assessed and the monolayer/toxin structure does not change with time after protein binding has saturated.
Published by Elsevier B.V.

Keywords: Neutron reflectivity; X-ray reflectivity; X-ray grazing incidence diffraction; Protein binding; Model biomembranes; X-ray beam damage

1. Background

Many bacterial toxins bind and gain entrance to target cells through specific interactions with membrane components. One such example is cholera toxin ($CTAB_5$), a pathologically active agent secreted by the bacterium *Vibrio cholerae* [1]. The toxin has an AB_5 arrangement of subunits. Five identical B subunits (CTB_5), each composed of 103 amino acids, form a pentameric ring with a vertical height of 32 Å and a radius of 31 Å [2,3]. CTB_5 is responsible for binding the toxin to its cell-surface receptor, ganglioside GM_1. The single A-unit is a disulfide-linked dimmer composed of an A1 and A2 subunit that is aligned through the central pore 'doughnut hole' of the B_5 subunit. After proteolytic cleavage (between residues 192 and 194) and reduction of the disulfide bond (cys187 = cys199), it has been proposed that the A1 peptide crosses the cell membrane and reaches the cytoplasmic face [4]. There, it interacts with integral membrane proteins, disrupting their normal function, resulting in a large efflux of water and ions from the cell (severe diarrhea) [5]. Although much is known about the structure and catalytic activity of cholera toxin, the mechanism by which cholera toxin crosses the plasma membrane remains unknown.

2. Experimental

2.1. Materials

Lipid monolayers were studied at the air–water interface using a Langmuir trough designed to fit at the horizontal reflectometer beamline (NG7) at the National Institute of Standards and Technology (NIST), Center for Neutron Research (NCNR, Gaithersburg, MD) and at the horizontal scattering diffractometer (BW1) at HASYLAB, Deutsches Elektronen-Synchrotron (DESY, Hamburg, Germany). The lipid monolayer was composed of 80:20 mole% of

* Corresponding author. Fax: +1 505 665 2676.
E-mail address: jarek@lanl.gov (J. Majewski).

0927-7765/$ – see front matter. Published by Elsevier B.V.
doi:10.1016/j.colsurfb.2004.10.009

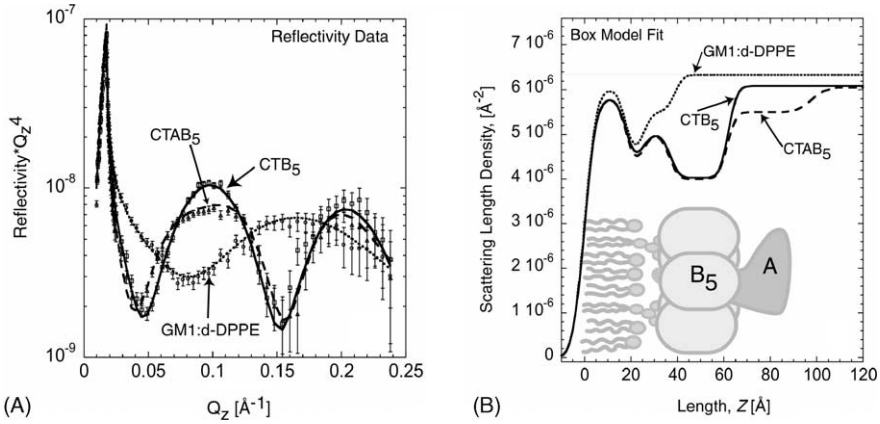

Fig. 1. Neutron reflectivity. (A) Neutron reflectivity of the monolayer, monolayer with bound CTB_5, and monolayer with bound $CTAB_5$. Points with error bars are measured data. Solid and dashed lines indicate fits to the data corresponding to the scattering length density profile in (B). (B) Scattering length density profile of box model fits shown in (A). A detailed schematic of the box model is provided in Fig. 2. In the profile for the monolayer, the lipid tail, head, and saccharide regions are clearly distinguishable. When CTB_5 and $CTAB_5$ are bound, the structure of the lipid monolayer is not significantly altered. The decrease in scattering length density ($\beta(z)$) of the lipid tail and headgroup regions is due to an increase in the area per molecule consistent with geometrical constraints applied when cholera toxin binds GM_1. The A subunit clearly resides below the B_5 pentamer, facing away from the lipid layer.

DPPE[1]:GM_1 [2-dipalmitoyl-*sn*-glycero-3-phosphoethanolamine:galactosyl-*N*-acetylgalactosaminyl (*N*-acetyl-neuraminyl) galactosylglucosylceramide (GM_1 ganglioside)]. GM_1 and DPPE were obtained from Avanti Polar Lipids[2] and were used without further purification. Cholera toxin $CTAB_5$ was purchased from BioMol Research Labs and CTB_5 was purchased from Sigma. D_2O was obtained from Cambridge Isotope Laboratories Inc. Lipids were dissolved in chloroform:methanol 90:10 (∼1.2 mg/mL), mixed to obtain a 80:20 mole ratio, and deposited on H_2O or D_2O buffer subphase (170 mM NaCl, 1.4 mM NaN_3, 0.3 mM EDTA, 15 mM Trizma–HCl, pH = 5.5–6.1). The molar composition of the monolayer, surface pressure of 20 mN/m, and temperature of 20 °C were held constant for all experiments reported here.

3. Results and discussion

3.1. Neutron and X-ray reflectivity

Reflectivity, *R*, is defined as the intensity ratio of neutrons/X-rays elastically and specularly scattered from a surface relative to the incident neutron/X-ray beam. When measured as a function of wave-vector transfer ($Q_z = |k_{out} - k_{in}| = 4\pi \sin \alpha/\lambda$, where α is the angle of incidence and λ the wavelength of the neutron/X-ray beam), the reflectivity curve contains information regarding the sample–normal profile of the in-plane average of the coherent scattering length densities, $\beta(z)$. In other words, reflectivity is sensitive to the average density structure normal to the interface. Analysis of the reflectivity profiles was performed by fitting real-space models to the measured reflectivity curve.

The experimentally measured neutron reflectivity profiles for (1) the mixed d-DPPE:GM_1 monolayer, (2) the monolayer with CTB_5, and (3) the monolayer with $CTAB_5$ on a D_2O subphase are shown in Fig. 1A. Box models of constant $\beta(z)$ based on the molecular structure of the molecules fit well to the experimental reflectivity profiles in all three cases. The results of these studies, shown in Fig. 1B, verify some structural features of the system. First, the GM_1 oligosaccharide region can clearly be seen extending 13 Å into the aqueous phase before toxin is bound, consistent with previous X-ray scattering studies [6]. Second, the B_5 subunit is clearly visible approximately 11 Å away from the lipid headgroup region when CTB_5 binds to the lipid monolayer. And third, the A subunit faces away from the lipid monolayer. Analogous results are observed from X-ray reflectivity experiments (results not shown), where the B_5 and A subunits were found to have the same orientation as determined from neutron reflectivity measurements Table 1.

In Fig. 2 difference profiles are calculated from the $\beta(z)$ profiles obtained in Fig. 1. A small decrease in density is observed in the lipid region before and after toxin binding. No difference is observed when comparing the lipid layer state with bound CTB_5 or $CTAB_5$. When subtracting the $\beta(z)$ profile of CTB_5 from the $\beta(z)$ profile of the monolayer, the B_5 subunit layer can clearly be seen attached to the monolayer. The scattering length density of the B_5 region is an average of bound toxin and D_2O subphase. The individual atom scattering lengths for the 515 amino acids (103 residues per B subunit) which make up CTB_5 plus 204 water molecules and the molecular volume ($V = 92{,}030$ Å^3 calc.) obtained from crystallographic data were used to calculate the scattering length density of CTB_5 [3]. Due to hydrogen–deuterium ex-

[1] Hydrogenated lipids were used in X-ray experiments. Lipids with deuterated tails were used for neutron experiments.

[2] Identification of a commercial product does not imply endorsement by the National Institute of Standards and Technology.

Table 1
Box model fitting scattering length densities for monolayers on D_2O[a]

Region	DPPE: GM_1 monolayer			With CTB_5			With $CTAB_5$		
	Z (Å)	$\beta(z) \times 10^{-6}$	σ (Å)[b]	Z (Å)	$\beta(z) \times 10^{-6}$	σ (Å)	Z (Å)	$\beta(z) \times 10^{-6}$	σ (Å)
Lipid tail	17.8 ± 2	6.0 ± 0.1	4 ± 1	17.8[c]	5.8	4[c]	17.8[c]	5.8	4[c]
Headgroup	7.5	4.5	3	7.5[c]	4.4	3[c]	7.5[c]	4.3	3[c]
GM_1	13.5	5.5	3	11.7	5.0	3[c]	11.2	5.0	3[c]
CTB_5				25	4.0	3	25[c]	4.0	3[c]
$CTAB_5$							36.3	5.5	3
Subphase[d]		6.3	3		6.1[d]	3[c]		6.1[d]	5
Area expansion with protein		N/A			$8 \pm 5\%$			$8 \pm 5\%$	

[a] χ^2 values were between 1.7 and 2.4 for box model fits reported in this table.
[b] Because our Q_z range was limited to 0.24 $Å^{-1}$, fitted parameters were not very sensitive to small changes in roughness. A minimum roughness of 3 Å was assumed due to capillary waves.
[c] Parameters that were fixed based on monolayer profile and not allowed to vary during the fitting procedure for $CTAB_5$ and CTB_5.
[d] The difference in the $\beta(z)$ of the subphase is due to the small addition of H_2O used for solvating the protein prior to incubation with the monolayer.

change and hydration changes, the $\beta(z)$ of CTB_5 in D_2O will be different than the $\beta(z)$ of CTB_5 in H_2O. A one-dimensional NMR spectrum was run on a CTB_5 sample to determine the percentage of hydrogen exchange with deuterium. NMR analysis showed that $5 \pm 3\%$ of the total hydrogen exchanged on the CTB_5 molecule when dissolved in D_2O during an hourly time scale. Based on the $\beta(z)$ of the B_5 region, the percentage coverage of CTB_5 was calculated to be $51 \pm 2\%$ in D_2O subphase (5% hydrogen–deuterium exchange) using Eq. (1):

$$\beta(z)_{\text{measured}} = (1 - X)(\beta(z)_{D_2O}) + 0.953(X)(\beta(z)_{CTB_5}) + 0.047(X)(\beta(z)_{D_2O \text{ in pore}}) \quad (1)$$

where X is the % coverage of CTB_5, $\beta(z)_{D_2O} = 6.1E{-}06$ $Å^{-2}$, and $\beta(z)_{CTB_5,D_2O} = 1.8E{-}06$ $Å^{-2}$, 0.0953 and 0.047 are the values obtained from the ratio of CTB_5 volume (92030 $Å^3$) to central pore volume (4580 $Å^3$). In $\beta(z)_{CTB_5}$ the scattering length of each atom was obtained from the NIST website http://www.ncnr.nist.gov/resources/n-lengths (C = 6.646 fm, O = 5.803 fm, N = 9.36 fm, S = 2.85 fm, H = −3.74 fm, D = 6.671).

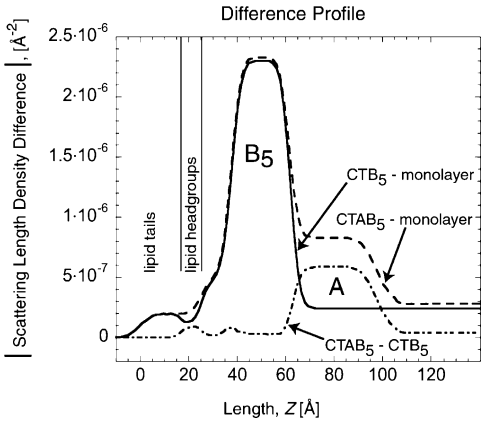

Fig. 2. Scattering length density difference profile of NR measurements done on D_2O buffer subphase. To create the difference profiles, the $\beta(z)$ profile of the pure monolayer was subtracted from the CTB5 and CTAB5 $\beta(z)$ profiles. In the CTB_5-monolayer case, the B_5 unit can be seen along with differences in the lipid region. In the $CTAB_5$–CTB_5 case, the A unit can clearly be seen to be oriented away from the lipid layer. In the CTAB–CTB5 difference profile, there is little to no change in the lipid region when either protein is bound.

3.2. X-ray grazing incidence diffraction (GID)

X-ray GID is a surface sensitive technique that allows the characterization of thin crystalline layers at an interface and has the ability to provide in-plane (lateral) structural information. During this procedure, X-rays are incident at an angle less than the critical angle for total reflection creating an evanescent wave that propagates laterally at the interface. This evanescent wave has an exponentially damped amplitude along the inward surface normal to the interface with a decay length of ∼100 Å. The evanescent wave is diffracted by lateral two-dimensional order in the monolayer or bound protein layer. If there is crystalline order, the evanescent wave may be Bragg scattered from a grain, which is oriented so its ($h\,k$) lattice 'planes' make an angle θ_{hk} with the incoming evanescent beam thereby fulfilling the Bragg condition, $\lambda = 2d_{hk} \sin\theta_{hk}$ [7]. It is possible to acquire diffraction peaks from both the lipid tails and the protein layer. The concentration of GM_1 receptor was sufficient to enable, two-dimensional cholera toxin crystals to assemble. Consequently, structural information can be deduced from both the lipid layer and the bound cholera toxin layer.

Fig. 3 shows Bragg diffraction peaks of both the lipid and protein layers. Results from qualitative analysis of these peaks are consistent with the neutron reflectivity results described above. The lipid peak of the monolayer is located at 1.49 $Å^{-1}$ before toxin is bound. This position in reciprocal space corresponds to a d spacing of 4.2 Å in real-space. At a surface pressure of 20 mN/m, the pure monolayer has a distorted hexagonal unit cell. When $CTAB_5$ or CTB_5 bind to the lipid monolayer, a decrease in intensity of the lipid peaks is observed. This is caused by the further distortion of the hexagonal lipid unit cell when cholera toxin constrains GM_1 molecules at its binding sites. This is consistent with an $8 \pm 5\%$ increase in the area per molecule as measured by

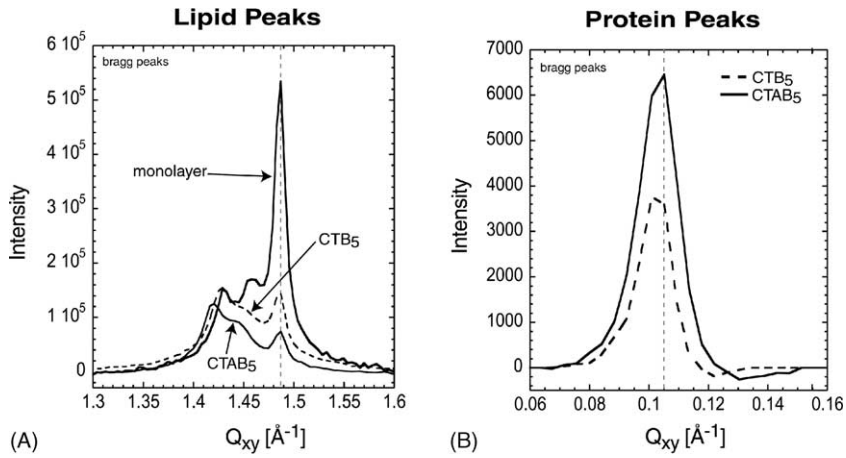

Fig. 3. (A) Three curves representing measured data for lipid diffraction peaks for: (1) the monolayer with bound toxin, (2) the monolayer with bound CTB_5, and (3) the monolayer with bound $CTAB_5$. When toxin binds, it can be seen that there is a decrease in Bragg peak intensity due to partial damage to the lipid crystal lattice. (B) Measured data for protein diffraction peaks for: (1) the bound CTB_5 layer, and (2) the bound $CTAB_5$ layer. The positions of the protein peaks correspond with a 61 Å *d* spacing consistent with a 62 Å B_5 unit diameter obtained from the three-dimensional crystal structure.

Langmuir trough expansion [8]. There are no significant peak shifts in Q_{xy} caused by toxin binding. At smaller Q_{xy} values (larger length scales), diffraction from the protein layer is observed. Protein peak positions ($Q_{xy} = 0.105$ Å^{-1}) correspond to a protein *d* spacing of 61 Å, consistent with a 62 Å diameter of the B_5 pentameric ring determined from the three-dimensional crystal structure [2,3]. When $CTAB_5$ or CTB_5 is enzymatically activated, there is a further decrease in the intensity of the lipid peaks (results not shown).

3.3. X-ray beam damage

Repeated exposure of the sample to the X-ray beam caused irreversible damage. Fig. 4A shows the reflectivity profiles of a 20% GM_1 80% DPPE monolayer that has been incubated with $CTAB_5$ for 1, 5 and 12 h. Each scan was performed on a region of the sample that had been previously scanned. It can be seen that the measured reflectivity profile undergoes significant changes with increased exposure. The corresponding electron density profiles (Fig. 4B) show a breakdown of the lipid monolayer and $CTAB_5$ structure. It was initially believed that this change in structure was due to real changes as the protein bound and penetrated the monolayer with time. However, measuring with neutron reflectivity showed no change in the reflectivity profile for repeated scans done over a 16.5 h incubation period. The neutron beam is not destructive to the sample due to its weak interaction with only atomic nuclei. Due to these results, we concluded that protein binding saturated after 3 h and changes with increased incubation time seen using X-ray reflectivity were solely a result

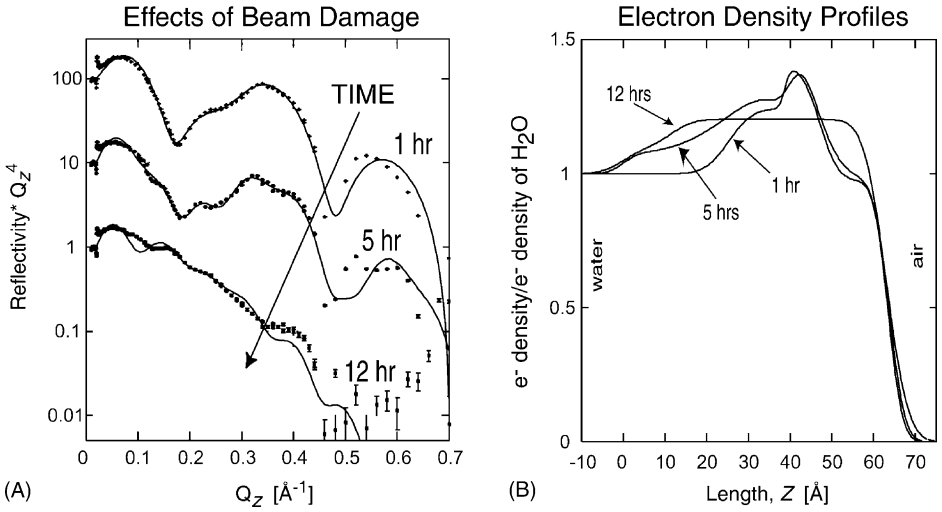

Fig. 4. Repeatedly scanned X-ray reflectivity measurements of a 20% $GM_1$80% DPPE monolayer that has been incubated with $CTAB_5$ for 1, 5 and 12 h. The result demonstrates the effects of beam damage on the sample. Neutron reflectivity results showed that this change in reflectivity with time was a consequence of beam damage to the sample.

of X-ray beam damage. In later X-ray reflectivity measurements, care was taken to minimize beam damage by translating the sample a distance perpendicular to the X-ray beam during scans proportional to the intensity of X-ray incident on the sample and only scanning a region of the sample once. A consecutive X-ray reflectivity measurement of a sample that has been properly translated showed no change with time after 3 h (or after saturation).

4. Conclusion

Using neutron/X-ray reflectivity we have successfully observed the cholera toxin protein layer specifically bound to a lipid monolayer containing ganglioside GM_1. The percentage area coverage of CTB_5 bound to the monolayer was calculated to be $51 \pm 2\%$. Using X-ray GID, we observed diffraction from the lipid tails and the protein layer. GID results show a decrease in diffraction intensity when $CTAB_5$ or CTB_5 bind. Qualitative analysis illustrates a decrease in lipid packing and distortion of the lipid unit cell when the toxin binds. This is consistent with an increase in area per molecule of the monolayer driven by toxin binding. Comparison of neutron and X-ray reflectivity showed that the monolayer/toxin structure does not change with time after protein binding has saturated.

Acknowledgments

This work was supported by the Searle Scholars Program/the Chicago Community Trust (01-L-108). The Manuel Lujan Jr., Neutron Scattering Center is a national user facility funded by the United States Department of Energy, Office of Basic Energy Sciences-Materials Science, under contract W-7405-ENG-36 with the University of California. We acknowledge the support of the National Institute of Standards and Technology, U.S. Department of Commerce, in providing the neutron research facilities used in this work. We acknowledge the support of HASYLAB, Deutsches Elektronen-Synchrotron (DESY, Hamburg, Germany) in providing the X-ray research facilities used in this work We gratefully thank Thorsten Dieckmann at the Chemistry Department, University of California at Davis for NMR spectrometer time and analysis.

References

[1] J.L. Middlebrook, R.B. Dorland, Bacterial toxins-cellular mechanisms of action, Microbiol. Rev. 48 (3) (1984) 199–221.
[2] R.G. Zhang, et al., The three-dimensional crystal structure of cholera toxin, J. Mol. Biol. 251 (4) (1995) 563–573.
[3] R.G. Zhang, et al., The 2.4 Angstrom crystal structure of cholera toxin B subunit pentamer-choleragenoid, J. Mol. Biol. 251 (4) (1995) 550–562.
[4] J.J. Mekalanos, R.J. Collier, W.R. Romig, Enzymic activity of cholera toxin. 2. Relationships to proteolytic processing, disulfide bond reduction, and subunit composition, J. Biol. Chem. 254 (13) (1979) 5855–5861.
[5] J. Holmgren, Actions of cholera-toxin and the prevention and treatment of cholera, Nature 292 (5822) (1981) 413–417.
[6] J. Majewski, et al., Packing of ganglioside-phospholipid monolayers: an X-ray diffraction and reflectivity study, Biophys. J. 81 (5) (2001) 2707–2715.
[7] J. Als-nielsen, et al., Principles and applications of grazing incidence X-ray and neutron scattering from ordered molecular monolayers at the air–water interface, Phys. Rep. 246 (5) (1994) 252–313 (Review).
[8] R. Faller, T.L. Kuhl, Modeling the binding of cholera-toxin to a lipid membrane by a non-additive two-dimensional hard disk model, Soft Mater 1 (3) (2003) 343–352.